

1489

176
11-20-78
DR. 749

NOVEMBER 1978

PPPL-1489

UC-20g

MASTER A METHOD FOR DETERMINING A
STOCHASTIC TRANSITION

BY

J. M. GREENE

**PLASMA PHYSICS
LABORATORY**



REPRODUCTION OF THIS DOCUMENT IS UNLIMITED

**PRINCETON UNIVERSITY
PRINCETON, NEW JERSEY**

This work was supported by the U. S. Department of Energy
Contract No. EY-76-C-02-3073. Reproduction, translation,
publication, use and disposal, in whole or in part, by or
for the United States Government is permitted.

—

assertions. These are consistent with all that is previously known, strongly supported by numerical results, and lead to a method for deciding the existence of any given KAM surface computationally.

I. INTRODUCTION

Problems in many branches of physics can be reduced to the study of two-dimensional measure-preserving mappings. In one important application, these mappings are an abstract representation of the simplest nontrivial problem of classical mechanics, the motion of two coupled oscillators.¹ It is an intriguing problem because the corresponding equations are simple and deterministic, with solutions that are either ordered or chaotic. The type of solution depends sensitively on both the parameters of the system and on the initial conditions. The aim of this paper is to illustrate a point of view for the examination of the boundaries between these types of motion. The method adopted here is to first explore the problem empirically with the aid of a computer, and then use this insight to guide analytic calculations.

A number of authors²⁻⁶ have recently written reviews of the subject covered in this paper, so that it need not be introduced in great detail. One physical example will be given here to provide a context for the remainder of this paper. Consider a particle constrained to the surface of a nonsymmetric bowl, i.e., moving in a potential $V(x,y)$ which has a minimum at $x=y=0$. In general, the particle will go around and around the bowl on some irregular

orbit. For ease in picturing and understanding this orbit, its dimensionality can be reduced by one by a method introduced by Poincaré. Consider a time at which the orbit crosses the ray $y = 0, x > 0$. This orbit is completely characterized by its position in the two-dimensional phase plane (x, \dot{x}) since the requirement $y = 0$ together with the conservation of energy can be used to complete the specification of the orbit in the full phase space. An orbit is then conveniently pictured through its successive intersections with this plane.

The orbits running around the bowl from intersection to intersection of the phase plane (x, \dot{x}) determine a mapping of the phase plane onto itself. By one of Poincaré's invariants, the area of a bundle of orbits is conserved in this mapping. Mappings with this area preserving property can be constructed analytically and these show the full range of orbit types as those arising from Hamiltonian differential equations. Thus, they represent a very convenient abstraction of dynamics, since they can be evaluated rapidly and accurately.

This paper is devoted to the study of a particular mapping that was introduced by Taylor,⁷ and more recently treated extensively by Chirikov.⁴ Termed "the standard mapping" by the latter author, it is

$$r_{n+1} = r_n - \frac{k}{2\pi} \sin 2\pi \theta_n ,$$

$$\theta_{n+1} = \theta_n + r_{n+1} . \quad (1)$$

It transforms a point (r_n, θ_n) to the point (r_{n+1}, θ_{n+1}) . In this space an orbit is a sequence of points generated by successive iterations of the mapping on an initial point (r_0, θ_0) . One iteration of this mapping is thus analogous to one traversal of the particle around the bowl in the previous example. For this reason, the number of iterations that generate an orbit segment will be called the length of that segment.

The mapping of Eq. (1) is naturally periodic in both θ and r with unit period. Thus, the domain $0 \leq r < 1$, $0 \leq \theta < 1$ will be treated as a torus.

Consider the standard mapping for the value $k=0$. Then r is a constant of the motion, and the mapping is integrable.⁸ Orbits on surfaces where r is rational close on themselves after a finite number of iterations of the mapping, and thus are periodic. Surfaces with irrational r are filled ergodically as the orbits are extended indefinitely.

Three typical orbit segments for nonvanishing k are shown in Fig. 1. Now a type of orbit appears that did not exist for the integrable case, one that apparently randomly fills out some area of the torus. These will be called stochastic, or two-dimensional orbits. Two such orbits are illustrated in Fig. 1. The two types of orbits that appeared in the integrable case are also found when k is finite. According to a theorem of Kolmogorov, Arnol'd, and Moser,^{9,10} for sufficiently small but finite k , there are orbits filling surfaces that in the limit as k vanishes go continuously into surfaces with irrational r . These are one-dimensional orbits, or KAM surfaces. Two orbits of this type are illustrated in Fig. 1. Finally,

according to a theorem of Poincaré and Birkhoff,⁵ surfaces with rational r are reduced to a finite number of periodic orbits when k is nonvanishing. In fact, in Appendix A it is shown that for this mapping two such orbits survive from each rational surface. These orbits can be called zero-dimensional. One orbit of this type is denoted by the symbol O in Fig. 1. The resultant mapping, then, is a complex mixture of zero-, one-, and two-dimensional orbits.

Two KAM surfaces extending around the r, θ torus in the θ direction divide the torus in two. This divides the orbits into two classes, since by continuity and uniqueness, orbits in one region cannot cross the bounding KAM surfaces into the other region. Under this circumstance, two stochastic orbits such as shown in Fig. 1 are distinct and disconnected. Thus, these orbits cannot wander around the torus in the r direction.

On the other hand, for sufficiently large values of k , orbits are seen to encircle the r, θ torus in the vertical, or r direction. This behavior will be called connected stochasticity. The presence of connected stochasticity precludes the existence of horizontally encircling KAM surfaces.

We are thus led to the following picture. For small values of k , there are many KAM surfaces that encircle the r, θ torus horizontally. These divide the space into many compartments, each of which may contain stochastic orbits. For larger values of k , there are fewer such KAM surfaces, and individual stochastic orbits can occupy a greater area of the phase space. Finally, at some critical value of k , the last horizontally encircling KAM surface disappears. For larger values of k there are vertically, encircling stochastic orbits. A major purpose of this paper is to calculate and describe

the critical k .

Previous work on this problem for this mapping has been summarized by Chirikov.⁴

The method of approach used in this paper was first studied several years ago.¹¹ It is based on an examination of the stability of periodic orbits. These orbits are attractive points of departure since they are of finite length, and thus can be treated with arbitrary accuracy. It is shown here that there is necessarily a close relation between the stability of these orbits and the existence of nearby KAM surfaces.

This paper is an improvement over the previous paper in several respects. The particular mapping studied here is superior. There is now a well-defined problem for finding the critical k for connected stochasticity that has no simple analog in the previous mapping. Also, this mapping is continuously connected to an integrable mapping through the parameter k , which is very useful conceptually. Among other developments that have been helpful is a new formulation of the problem of calculating the stability of periodic orbits given by Bountis and Helleman¹² that sheds considerable new insight. This is discussed in the next section, and described in more detail in Appendix B. Finally, present computers have permitted the calculation and sifting of much more data, allowing stronger statements of results to be given.

The quantities to be calculated in this paper are defined and discussed in Sec. II. The results of many numerical calculations are then distilled into a series of assertions given in Sec. III. Some of the evidence leading to these assertions is given in Sec. IV.

Finally, the meaning of it all is discussed in Sec. V.

II. DEFINITIONS

The material in this section has considerable overlap with similar material in the previous paper.¹¹ It is included here for completeness, and also to point out certain differences between these two papers.

Here we are interested particularly in the periodic orbits of the mapping given in Eq. (1). A periodic orbit is a finite set of points that transform among themselves under iteration of the mapping, and all of which are accessible from any one of the points. We will say that the orbit is of length Q if the orbit closes after Q iterations.

Not all of the periodic orbits are considered here. The class of interest can be defined succinctly as those periodic orbits that exist for all values of the parameter k , down to $k=0$. Some of the other periodic orbits bifurcate out of shorter periodic orbits at a finite value k , and some just suddenly appear as k is increased. One way of classifying all these orbits is through the bifurcation tree that produced them, as k is varied from zero. This classification was called a hierarchy in the previous paper. Hopefully, it is somewhat clearer here, where the mapping can be connected to an integrable mapping by a continuous transformation, i.e., through variation of k .

A method for calculating all the periodic orbits of interest is given in Appendix A.

Similarly, attention in this paper is focussed only on those KAM surfaces that encircle the torus. Other KAM surfaces bifurcate out of periodic orbits, interspersed with the bifurcated periodic

orbits discussed above. These, however, provide only limited impediment to the diffusion of many orbits, since they do not encircle the torus. The KAM surfaces of interest can also be defined as those that exist down to $k=0$. The conclusion of this paper is that there is a close connection between the KAM surfaces and the periodic orbits that exist together down to $k=0$.

By extension, the KAM surfaces that bifurcate out of a periodic orbit are related to the interspersed periodic orbits that successively bifurcate out of the given orbit. All of the periodic orbits and KAM surfaces on a given branch of a bifurcation tree should be considered together as a system.

It is convenient to associate a winding number with the periodic orbits and KAM surfaces of interest. In the integrable limit, $k=0$, this winding number is $q=1/r$. For rational r , $r=P/Q$ with P and Q relatively prime, Q is the length of the orbit before it closes, and

$$P \equiv \sum_{n=1}^Q r_n = \sum_{n=1}^Q (\theta_n - \theta_{n-1}) = \theta_Q - \theta_0 \quad (2)$$

where r_n and θ_n are the coordinates of the n^{th} point of the periodic orbit. Then, from Eq. (1), P and Q , and thus

$$q \equiv Q/P \quad (3)$$

are well-defined and independent of k , and can be used to identify a given periodic orbit. Returning to the picture used in the

Introduction where an iteration of the mapping was analogous to a traversal of a particle once around a bowl, Q can be regarded as an angle, and it is reasonable to call q a winding number. This winding number can be extended to KAM surfaces in the obvious way.

The nature, behavior, and characteristics of periodic orbits and KAM surfaces are not continuous functions of the winding number, q . It is observed that, in the neighborhood of a given periodic orbit, KAM surfaces and other longer periodic orbits are strongly perturbed. In perturbation theory, this effect appears to be a problem of small denominators, where the denominator is a measure of the distance between a perturbing periodic orbit and the region of interest. A good way to take account of this phenomena is to express winding numbers as continued fractions,¹³

$$q = a_0 + \frac{1}{a_1 + \frac{1}{a_2 + \dots}} \quad (4)$$

where, since $q \geq 1$, the a_n 's are positive integers. This will be denoted

$$q = [a_0, a_1, a_2, \dots, a_N] \quad (5)$$

Note that $[a_0, a_1, a_2]$ approaches $[a_0, a_1]$ when a_2 becomes large. Thus, the magnitude of the partial quotients, a_n , is a measure of the degree of isolation of the associated orbit.

The continued-fraction representation is unique up to an ambiguity in the last partial quotient

$$[a_0, a_1, \dots, a_N] = [a_0, a_1, \dots, a_N - 1, 1] \quad (6)$$

as can be seen from the definition. There is also an inversion symmetry around the midpoint of the standard mapping, with the result that orbits with winding numbers q and $q/(q-1)$ are essentially identical. In the continued fraction representation, this means that winding numbers $[a_0, a_1, \dots, a_N]$ and $[1, a_0^{-1}, \dots, a_N]$ are interchangeable. It is amusing that this is symmetric with the natural ambiguity of continued fractions.

It is sometimes useful to place a subscript on q to indicate the number of partial quotients in its continued fraction representation.

Irrational numbers have unique representations as continued fractions, with an infinite number of partial quotients.¹³ Thus, these numbers will be denoted q_∞ . Successive truncations of the infinite continued fraction yield rational approximations that are called the convergents¹³ of q . These convergents yield, from among the periodic orbit of the given length or shorter, the one that most nearly approaches the surface of interest.

Other parameters can be calculated to further characterize the periodic orbits. Orbits in the immediate vicinity of the given orbit can be computed in the linear, differential approximation. The domain of this approximation is called the tangent space. It was well treated in the previous paper,¹¹ but the results will be summarized here.

The tangent space orbit $(\delta r_n, \delta \theta_n)$ at the point (r_n, θ_n) is given in terms of the initial conditions on the orbit $(\delta r_0, \delta \theta_0)$ at the point (r_0, θ_0) , through a matrix M ,

$$\begin{pmatrix} \delta\theta_n \\ \delta r_n \end{pmatrix} = M \begin{pmatrix} \delta\theta_0 \\ \delta r_0 \end{pmatrix} . \quad (7)$$

This matrix M can be computed as the product of matrices, one for each orbit section. Over the full cycle of a periodic orbit,

$$M = \prod_{i=1}^Q \begin{pmatrix} 1 - k \cos 2\pi \theta_i & 1 \\ -k \cos 2\pi \theta_i & 1 \end{pmatrix} . \quad (8)$$

The property of M of greatest interest is its eigenvalues. These are the Floquet multipliers for the linear difference equation in the periodic tangent space. From the area-preserving property of the mapping,

$$\text{Det } M = 1 , \quad (9)$$

the eigenvalues of M depend only on its trace. As will be seen, to obtain the best analytic properties it is convenient to subtract 2 from the trace, and then it is convenient to scale it with a factor of -4. This leads to a definition of a quantity to be called the residue,¹¹

$$R = \frac{1}{4}(2 - \text{Trace } M) \quad (10)$$

The eigenvalues of M are given in terms of the residue by

$$\lambda = 1 - 2R \pm 2[R(R-1)]^{1/2} . \quad (11)$$

When

$$0 < R < 1 , \quad (12)$$

the eigenvalues are complex with magnitude unity. Under this condition, tangent space orbits, continued over many periods, rotate about the origin on ellipses. If we express

$$\lambda = \exp i\alpha , \quad (13)$$

then α is the average angle of rotation per period. It is given in terms of the residue,

$$R = \sin^2 \alpha / 2 . \quad (14)$$

When $R < 0$ or $R > 1$, tangent space orbits lie on hyperbolae. Then the periodic orbit is said to be unstable since all the tangent space orbits march off to infinity, except those lying on the eigenvector of M with an eigenvalue less than one.

In the previous paper¹¹ a theorem of Poincaré's was invoked to show that, for each rational q , there are as many periodic orbits with positive residue as there are with negative residue. It follows from the results of Appendix B that, for the mapping treated here, there is always one orbit of each kind when k is small. These two periodic orbits with the same q will be distinguished by \pm superscripts.

For integrable mappings, all except a small, finite number of periodic orbits lie on surfaces composed of periodic orbits. Then there must be a line of periodic orbits in the tangent space also. A necessary condition for this is $R=0$ ($\lambda=1$). Thus, for the present mapping, all the residues for the periodic orbits of interest here vanish in limit as k goes to zero.

The positive residue orbits are stable when k is small, but the residues are seen to increase with k and ultimately become larger than unity. At that point the corresponding orbits become unstable. This change in orbit character, from stable to unstable, as k is increased, is the central concept of this paper that will be related to the disappearance of KAM surfaces.

Appendix B presents a result of Bountis and Helleman,¹² that the residue can also be written as the determinant of the $Q \times Q$ matrix,

$$R = -\frac{1}{4} \text{Det } H \quad (15)$$

$$H = \begin{pmatrix} 2 - k \cos 2\pi \theta_1 & -1 & \dots & -1 \\ & -1 & 2 - k \cos 2\pi \theta_2 & \\ & 0 & & \\ & \dots & & \\ -1 & & & 2 - k \cos 2\pi \theta_Q \end{pmatrix} \quad (16)$$

where H is tridiagonal with additional -1 's in the corners.

It is apparent that when k is large, the residue is proportional to k^Q . To prove this, one would need only to establish that periodic orbits do not approach either $\theta = 1/4$ or $\theta = 3/4$, and numerically the opposite tendency is observed.

In Appendix B it is shown that in the limit of small k also, the residue is proportional to k^Q .

In the succeeding sections of this paper, the aim is to make

sensible statements relating the residues of neighboring periodic orbits of different lengths. Since it appears that the magnitude of the residues is dominated by an exponential dependence on orbit length, it is natural to introduce a new quantity proportional to the Q^{th} root of R . The new quantity will be called the mean residue, f ,

$$f \equiv (|R|/\beta)^{1/Q} . \quad (17)$$

The quantity β could be adjusted for convenience, as is discussed in Sec. IV C. From the considerations of Sec. IV E, the value $\beta = 1/4$ is preferred for the cases of most interest, and that value has been used for all the numerical computations of this paper.

In the previous paper,¹¹ a slightly different definition of f was used, which was the square of the value used here. For the present mapping, it is clear that it is preferable to have f proportional to the perturbation k , rather than its square. In retrospect, this argument should have led to the present definition of f in the previous paper also.

A quantity partially related to the mean residue has been used by other authors,

$$h \equiv \frac{1}{Q} \ln |\lambda| \quad (18)$$

where λ is the eigenvalue of Eq. (11). When the residue is large, and therefore the eigenvalue is large,

$$\lambda \approx -4R \quad (19)$$

so that

$$h \approx \ln f . \quad (20)$$

However, in distinction to h , f is a real analytic function of k for both large and small values of k , and is thus considerably more useful in the same way that the residue is more useful than the eigenvalue.

The quantity f can be evaluated for both positive and negative residue orbits. A superscript \pm will be used to indicate the sign of the residue of the orbit.

One further property of the tangent space mapping is useful, that of the shapes of the conic section surfaces that are invariant when the mapping is extended over a full period. Since this quantity depends on more than the trace and determinant of M , we introduce the parameterization,¹¹

$$M \equiv \begin{pmatrix} a+d & c+b \\ c-b & a-d \end{pmatrix} . \quad (21)$$

The condition on the determinant of M can be written

$$a^2 + b^2 - c^2 - d^2 = 1 . \quad (22)$$

First consider unstable periodic orbits so that the invariant surfaces are hyperbolae. It is straightforward¹¹ to establish that the angle γ between the asymptotes of these hyperbolae is given by

$$\tan^2 \gamma = \frac{a^2 - 1}{b^2} = \frac{4R(R-1)}{b^2} \quad (23)$$

Thus, when the residue is small, the hyperbolae degenerate into straight lines, appropriately for integrable systems.

Further, it can be shown that in the stable case, where the invariant conics are ellipses, the same expression is related to the ratio of major, ρ_+ , to minor, ρ_- , semi-axes,

$$\frac{4\rho_+^2 \rho_-^2}{(\rho_+^2 + \rho_-^2)^2} = \frac{1 - a^2}{b^2} = \frac{4R(1-R)}{b^2} \quad (24)$$

Again, small values of R show the approach to the straight lines of an integrable system.

III. ASSERTIONS

An outline of the numerical results that have been obtained for the standard mapping is given in this section. The results are presented as a series of assertions, or hypotheses. The evidence for the truth of these assertions will be given in the succeeding section. The emphasis here is on their significance, and on the relation between them. It will be seen that they are not independent, but since they have not been proven, it is undesirable to form a logical structure that is too rigid.

Assertion I

$$k \leq f \leq 1 + \frac{1}{2}k + \frac{1}{2}(k^2 + 4k)^{1/2} ,$$

$$\frac{\partial f}{\partial k} \geq 1 , \quad f^+ < f^- .$$

This first assertion applies to each periodic orbit and provides some estimates and bounds on the magnitude of f . In fact, for the standard mapping, f is close to linear in k . According to the third part of this assertion, the periodic orbit with negative residue has a slightly larger value of f than the associated orbit with positive residue. Note that the upper bound on f is consistent with the bound on the derivative.

Assertion II: Consider the mean residue, f , to be a function of the partial quotients of the continued-fraction representation of the winding number q of a given periodic orbit. Then

$$f(a_0, \dots, a_i, \dots, a_N) > f(b_0, \dots, b_i, \dots, b_N)$$

if $a_i = b_i + 1$ for some set of b_i 's that satisfy $b_i \approx b_{\max} = \max_j (b_j)$, and $a_i = b_i$ otherwise, with the further restriction

$$a_0 = a_N = 1 .$$

Further,

$$\lim_{a_i \rightarrow \infty} f(a_0, a_1, \dots, a_i, \dots, a_N) > 1 .$$

This assertion compares orbits whose continued-fraction representations have the same number of partial quotients, and says that the mean residue is increased if any of the largest partial quotients are increased.

The first comment to be made about this assertion is that it is reasonable to consider f to be a function of the partial quotients of q rather than a function of q directly. In fact, f is not a well organized function of q with continuity properties. Its dependence on the partial quotients is more orderly. The general thrust of this assertion is that periodic orbits with large partial quotients have large values of f , and thus tend more to instability. In other words, periodic orbits that are close to shorter periodic orbits tend to be more unstable than orbits that are further removed.

Unfortunately, the mean residue is not simply monotonic with respect to each partial quotient. Thus, the desired properties must be expressed in terms of some weaker statement. The most important use of a statement of this kind is the identification of the orbit

with the minimum value of f , among all those with a given number of partial quotients in the continued-fraction expansion of its winding number. This provides a context, for example, for Assertion IV below. This Assertion II seems to be the cleanest statement that is both true and useful in this respect.

The symmetries associated with the partial fraction representation permit the restriction on a_0 and a_N without eliminating any significant periodic orbit. Again, unfortunately, this restriction is necessary to avoid counterexamples.

The last part of this assertion, when combined with Assertion VI, leads to the conclusion that there is a stochastic region in the immediate vicinity of every chain of periodic orbits. Note that the bounds of Assertion I are consistent with the present inequality, and prevent the limit from diverging.

Assertion III: Consider an irrational winding number q , and its unique continued-fraction representation. Associated with this, consider the series of periodic orbits whose winding numbers are given by the successive truncations, or convergents, of this continued fraction, and calculate the mean residue for each. Then

$$f(q_\infty) \equiv \lim_{N \rightarrow \infty} f(q_N)$$

converges nontrivially, where

$$q_N \equiv [a_0, a_2, \dots, a_N] \quad .$$

Further,

$$f^+(q_\infty) = f^-(q_\infty) \quad .$$

This assertion continues the definition of $f(q)$ to irrational values of the argument. According to the theory of continued fractions, the orbits that have been used in each approximation have the minimum separation from the chosen irrational orbit among all orbits of a given length. This has a clear meaning, at least, when there is a KAM surface with the chosen irrational q . Thus, the irrational is approached through a consistent sequence of rationals.

The statement that the convergence of f is nontrivial means $f(q_\infty, k)$ is not identically unity. In that case, the interesting behavior associated with irrational winding numbers would be exhibited by some other function of the residue.

The second part of this assertion states that the same value of f is achieved if the limit is taken using either the positive or negative residue orbits. While according to Assertion I, the negative residue orbit yields the larger value of f for each finite approximation, the difference disappears in the limit. The significance is that near the irrational surface, associated positive and negative residue orbits will have the same character. See also the comments under Assertion VI.

Assertion IV: Define

$$q_\infty^* \equiv [1, 1, 1, \dots] = \frac{1}{2}(1 + \sqrt{5}) \quad .$$

Then

$$f(q_{\infty}^*) < f(q_{\infty}) \quad \text{for all} \quad q_{\infty} \neq q_{\infty}^* .$$

The irrational number q_{∞}^* has been known for millenia as the golden mean. It has many interesting properties that are discussed in Niven,¹³ and also by Gardner.¹⁶ It is the number that is least easily approximable by rationals. It is thus the point at which the problems of small denominators are minimal, and the surface for which the conditions for the KAM theory are most easily satisfied.

Assertion IV follows if Assertion II is true for all sets of orbits with a finite number of partial quotients. Together with Assertion VI, it yields Assertion VII for the boundary of connected stochasticity for this mapping.

The details of this assertion are true only for the standard mapping considered in this paper. It should be borne in mind that the partial quotients determine the position of the orbit with respect to inhomogeneities over the full domain of the mapping, as well as its relation to nearby shorter periodic orbits. The former variations will always have a weak dependence on the partial quotients a_i with large i . Thus, this assertion should be relevant, for general mappings, for all except the first few partial quotients. See also the comments on the next assertion.

Assertion V: Consider an irrational winding number q_{∞}^+ whose partial fraction representation has the property

$$a_i = 1 \quad \text{for all} \quad i \geq N .$$

Choose that value of $k = k_C^+$ such that the converged mean residue satisfies

$$f(q_\omega^+, k_C^+) = 1 .$$

Then the associated residue converges with the limit,

$$R(q_\omega^+, k_C^+) = 0.25 .$$

This assertion can be approached in the following manner. Consider an asymptotic representation of the residues and mean residues for the sequence of convergents of a particular q_ω , in the limit of a large number of partial quotients. The length Q of the associated periodic orbits can be taken to be the large parameter of the expansion. According to Assertion III, this asymptotic expansion for the residues can be written

$$R \approx \gamma(Q, q_\omega, k) f^Q(q_\omega, k) [1 + \dots] , \quad (25)$$

where γ need only satisfy

$$\gamma^{1/Q} \xrightarrow{Q \rightarrow \infty} 1$$

Then Assertion V can be restated

$$\gamma(q_\omega^+, k_C^+) = 0.25 \quad (26)$$

The irrational numbers q_{∞}^+ are closely related to the golden mean that appeared in the previous assertion. They are an obvious generalization when attention is fixed on a subregion of a given mapping. It is remarkable that this assertion appears to be true for all such numbers, even though there are counterexamples to its generalization to the full set of irrational numbers. Since the surfaces corresponding to the winding numbers q_{∞}^+ have a considerable variation in their immediate environment, there is some hope that this assertion could be generalized to other mappings.

Picking up a loose end, the rather arbitrary value $\beta = 1/4$ that appears in the definition of f , Eq. (17), has little or no influence on the assertions of this section. Only in Assertions I and II will this number enter, and then, rather weakly.

The significance of this Assertion V is in determining a best value for β . A value of $1/4$ yields the most rapid convergence, in the sense of Assertion III, for those interesting winding numbers q_{∞}^+ in the vicinity of the critical limit, $k = k_c$, since the asymptotic expansion for the mean residue, from Eqs. (17) and (25), is

$$f = (\gamma/\beta)^{1/Q} f(q_{\infty}) [1 + \dots] , \quad (27)$$

and the leading term is independent of Q only when $\beta = \gamma$.

It is interesting that in the preceding paper, similar

considerations, if less coherently presented and less accurately evaluated, led also to the conclusion that β should be given the value of $1/4$ for the most rapid convergence. It is very tempting to speculate that, for some hidden reason, $\beta = 1/4$ is universally the desired value to best determine the KAM surfaces of most interest. The common factor between the corresponding orbits is not at all clear.

Assertion VI: The KAM surface with a given winding number q_∞ exists if and only if

$$f(q_\infty) < 1 .$$

This is perhaps the most striking of the various assertions of this section. An intuitive feeling for this assertion can be gleaned from a consideration of the definition of f , Eq. (17). When $f(q_\infty)$ is slightly smaller than unity, Assertion III yields the conclusion that the necessarily long, nearby periodic orbits corresponding to the convergents of q_∞ will all have a small residue, $|R| \ll 1$. On the other hand, when $f(q_\infty)$ is slightly larger than unity, these residues will be large, $|R| \gg 1$. Thus, at the critical value of k , $R(q_\infty, k)$ will have an infinite discontinuity. It should not be surprising that this discontinuity is associated with other remarkable phenomena. Note that, from Assertion III, this discontinuity occurs simultaneously for positive and negative residue orbits.

Assertion VII: Connected stochasticity occurs for

$$k > k_C^*$$

where

$$f(q_{\infty}^*, k_C^*) = 1 \quad , \quad k_C^* = 0.971635...$$

From Assertion IV,

$$f(q_{\infty}, k_C^*) > 1 \quad , \quad \text{for all } q_{\infty} \neq q_{\infty}^* \quad ,$$

and thus, from Assertion VI, no other KAM surfaces exist that encircle the torus horizontally in the usual pictorialization. Therefore, for $k > k_C^*$, there are no impediments to orbits encircling the torus vertically. Evidence will be presented that this latter type of orbit does exist, then, at least for k 's that are slightly above the critical value. That is, it is shown that there is at most a very small range of the parameter k for which there is neither a vertically encircling stochastic type orbit, nor a horizontally encircling KAM orbit. This is sort of reasonable in the following sense. If there are no vertically encircling orbits, then each orbit must have some upper and lower bound,

$$r_L(\theta) < r_i < r_U(\theta) \quad .$$

These bounds can be intuitively identified with KAM surfaces.

IV. EVIDENCE

A. Assertion I

The upper limit on f has been obtained by considering the Jacobian matrix M of Eq. (8). For any given length orbit, the trace of this matrix must always be less in absolute magnitude than the trace of the matrix obtained from an orbit restricted to $\theta = 1/2$, i.e.,

$$|\text{Trace } M| < \text{Trace} \begin{pmatrix} 1+k & 1 \\ k & 1 \end{pmatrix}^Q = \lambda^Q + \lambda^{-Q} \quad (28)$$

The inequality follows from the fact that the product of matrices on the right then involves the sum of positive terms, each of which has been maximized over conceivable orbits. The trace on the right has been evaluated by diagonalization, and thus represented in terms of the largest eigenvalue of each factor,

$$\lambda = 1 + \frac{1}{2}k + \frac{1}{2}(k^2 + 4k)^{1/2} \quad (29)$$

When this estimate is used with the definition of f , an upper bound is obtained that decreases with orbit length. Since the general trend of Assertions II and III is that f does not decrease with the orbit length, the leap has been made to minimize this bound over Q , with the result given in Assertion I.

A few periodic orbits are independent of k . Thus, they are easily found. For $q=1$, the positive residue orbit is

$$r = 0, \quad \theta = 0 \quad (30)$$

and the negative residue orbit is

$$r = 0, \quad \theta = \frac{1}{2} \quad (31)$$

The corresponding mean residues are easily evaluated yielding

$$f^{\pm}(1,k) = k \quad (32)$$

Similarly, the positive residue orbit for $q=2$ is

$$r = \frac{1}{2}, \quad \theta = 0; \quad r = \frac{1}{2}, \quad \theta = \frac{1}{2} \quad (33)$$

and the corresponding mean residue is

$$f^{\pm}(2,k) = k \quad (34)$$

These orbits thus test the lower bound on f and its derivative.

The expansion for small k given in Appendix B can yield as many asymptotic values of f as one cares to evaluate. In this limit, the positive and negative residue orbits yield the same mean residues. A few such values are

$$f(3) = (9/8)^{1/3} k$$

$$f(4) = (5/3)^{1/4} k$$

$$f(5) = [(1675 + 375\sqrt{5})/768]^{1/5} k$$

$$f(5/2) = [(1675 - 375\sqrt{5})/768]^{1/5} k \quad (35)$$

Finally, in Table I, a few values of the mean residue are given for orbits with the winding number $q = 3$.

Altogether, the results of this subsection should provide some feeling for the typical behavior of f as a function of k . The most noteworthy result is that the positive residue increases monotonically as a function of k . It passes through unity, and thus the orbit becomes unstable without hesitation or indication of nonanalyticity in these parameters.

B. Assertion II

In Table II, a series of values of mean residue is presented for a number of orbits whose winding number q has five partial quotients. It is seen that minimizing the partial quotients yields the minimum mean residue. On the other hand, the fifth in the list is smaller than the second. This shows the difficulty of making useful true statements, without invalidating Assertion II.

The limit of a given partial quotient tending to infinity that is considered in the second part of this assertion is quite interesting. The winding number in this limit approaches the continued fraction that is truncated at the term $i-1$, as is clear from the continued fraction representation. Experimentally, the corresponding limiting

orbits are closely associated with the negative residue orbit with the truncated winding number. This latter orbit will be referred to as the truncated orbit. It is observed that the limiting orbit approaches the homoclinic points of the truncated orbit¹⁷ where each set of homoclinic points is defined as an orbit of infinite length that asymptotically, at either end of its trajectory, approaches points of the truncated orbit.⁵ Thus, orbits that are close to the truncated orbit at several points will also be close to corresponding homoclinic points.

Now consider a set of limiting orbits with increasing partial quotients, as in the second part of Assertion II. These have an increasingly long residence near the truncated orbit with short bridges from one orbit section to the next. The beginning of this process can be seen in Fig. 3 of Ref. 11. The contributions to the Jacobian matrix M from orbit sections neighboring the truncated orbit can be calculated as powers of the Jacobian matrix associated with the truncated orbit, and the contribution from the bridges is independent of a_i , when a_i is large. As a result,

$$R(q = Q/P) \approx (\lambda_t^{Q/Q_t} + \lambda_t^{-Q/Q_t})c \quad (36)$$

and

$$\lim_{a_i \rightarrow \infty} f(a_n) = (\lambda_t)^{1/Q_t} \quad (37)$$

where λ_t is the largest eigenvalue of the truncated orbit, Q_t is the length of that orbit, and c is a constant, for large a_i ,

associated with the bridges. Since the eigenvalue λ_t is always larger than one, the limiting f is also larger than one.

C. Assertion III

Table III presents data relating to the convergence of the mean residue f for a sequence of convergents to the golden mean. These have been chosen because the golden mean is the winding number of the greatest interest. The value of k given here is the best approximation to the critical k that has been evaluated. Attention for the moment should be focussed on the mean residue f , to the exclusion of R . It has been evaluated for both positive and negative residue points.

For the positive residue orbits, the convergence is oscillatory and the differences decrease approximately as Q^{-2} . Since Q increases exponentially from convergent to convergent as powers of the golden mean, the convergence of f is quite rapid and convincing.

The negative residue orbit exhibits convergence from above, and the differences decrease more slowly and they are more nearly proportional to Q^{-1} . The problem is that the value of β in the definition of f has been chosen to maximize the convergence of the positive residue orbit. For this set of orbits, the quantity γ of Eq. (25) is slightly larger than 0.25, as can be seen from Table III. A slightly larger value of β would provide faster convergence, without affecting the converged value, $f^-(q_\infty^*)$. Note also that, to within the limits of accuracy of the calculation, the converged f 's for the positive and negative residue orbits are identical.

As a further example, in Table IV the golden mean is again considered, but for a somewhat smaller value of k . Again monotonic convergence with differences proportional to Q^{-1} is observed. It thus appears that the optimizing β should be a function of k as well as of the orbit.

Part of the reason for the excellent convergence of these cases lies in the regularity of the succeeding partial quotients. Orbits with random partial quotients are probably less interesting in light of Assertion II, and they are more difficult to calculate. The problem is that orbits become long very fast, there is a limited window

$$10^{-10} < |R| < 10^9$$

within which residues can be calculated accurately because of roundoff, and the residue depends exponentially on orbit length.

There are a couple of possibilities for generalizing the results that have been given here. Perhaps the convergence of $f(q_{\infty}^*)$ could be combined with the approximate monotonicity of f with partial quotients discussed in Assertion II, and the upper bound established in Assertion I, to establish convergence in more general cases. Also, it might be possible to use the calculation of Appendix II to establish convergence in the limit of small k .

To conclude, the evidence for convergence seems quite strong for the interesting cases associated with the golden mean. It is at least credible that there should be convergence in a large generalization of this class.

D Assertion IV

No independent work has been done for this assertion. All the evidence assembled for Assertion II indicated that golden mean convergents yielded the smallest f , among all orbits whose winding number had a partial fraction representation with a given number of partial quotients. While this assertion follows from Assertion II, it is logically independent of the efforts to generalize it beyond the golden mean convergents. It has thus been given a separate number.

E Assertion V

Some evidence for this assertion has been given in Table III. The fact that the positive residue converges to $1/4$, accurate to at least four decimal places, is sufficiently remarkable to invite speculation that an integer is involved.

This inspired the calculation presented in Table V. Here an irrational winding number has been chosen whose first few partial quotients are arbitrary, but all of whose succeeding partial quotients are unity, $q = [3, 1, 4, 1, \dots] = (143 + \sqrt{5})/38$. Again, k has been carefully selected to be close to the critical value for this winding number. The associated residue here is also approaching $1/4$ to a remarkable degree of accuracy.

F Assertion VI

The evidence for this assertion is given in Figs. 2, 3, and 4.

In each of these figures, portions of periodic orbits have been plotted, with x's denoting negative residue orbits and o's denoting positive residue orbits. In every case, the orbits chosen are golden mean convergents.

For Fig. 2, the value $k=0.95$ has been chosen, and the corresponding mean residue has been evaluated,

$$f(q_m^*, 0.95) \approx 0.977$$

so that the golden mean KAM surface is expected to exist. In Fig. 2a the orbits shown have winding numbers $q = 55/34$ and $89/55$ respectively. These two numbers are slightly larger and smaller respectively, than the golden mean, and thus, the two orbits should enclose the golden mean KAM surface. This statement is true of the succeeding pairs of orbits also.

The next two golden mean convergents are shown in Fig. 2b. Each successive golden mean convergent orbit has approximately ϕ times as many points as the preceeding, where the golden mean is denoted by ϕ for brevity. Thus, the horizontal scale has been expanded by approximately ϕ^2 between Figs. 2a and 2b, and also between succeeding frames. This accounts for the fact that each figure exhibits about the same number of points.

When examining the bottom of a parabola with increasing magnification, the vertical scale should be expanded as the square of the expansion of the horizontal scale to preserve the aspect. Thus, for each succeeding frame in this figure, the vertical scale has been expanded by ϕ^4 .

This figure then, is entirely consistent with the picture that these successive convergent orbits are closing down on a KAM surface that is represented very well by the first few terms of its Taylor expansion.

Expressions for the mapping in the tangent space of these periodic orbits are given in Eqs. (23) and (24). Since R is very small and of the order 10^{-20} for the orbits of Fig. 2f, the invariant ellipses associated with the positive residue orbit are extraordinarily long and thin, with an aspect ratio of the order 10^{10} . Also, there is an extraordinarily small angle between asymptotes of the hyperbolae associated with the negative residue orbits. Even on the expanded scales used here, these figures are not resolvable from straight lines. Further, from Eq. (14), of the order of 10^{10} iterations are required to traverse these ellipses. Thus, about the same number of iterations would be required to distinguish the mapping in the portion of phase space delimited by Fig. 2f from the shear mapping of an integrable system.

Turn now to Fig. 3, which is very similar to Fig. 2, except that here $k = 0.971635$, which is the critical k to the accuracy of this figure. Remarkably unlike the previous picture, here a new structure appears with each successive magnification. From Table III, it can be seen that each of these orbits has very nearly the same residue, R . Thus, from Eqs. (23) and (24), the shape of the tangent space conic sections varies only with the parameter b . Evaluating this, it was found that these shapes would be similar from frame to frame, if the mean vertical magnification were 6.01/frame when averaged over a three-frame period.

This was used here, rather than the magnification of $\phi^4 = 6.85/\text{frame}$ used in the previous figure. It is seen that similarity is indeed achieved by this scaling. It seems natural to associate the structure on successive scales with a necessity to accommodate the invariant ellipses surrounding each stable orbit.

As further evidence in this direction, note that the threefold period in the structure is accompanied by a threefold period in the positions of the x and o points, relative to the center of each frame.

After carefully observing that Figs. 3c and 3f each exhibit two w shaped curves, one lying above the other, the picture emerges that the convergents for this value of k are squeezing down on some nonanalytic curve that has a structure on every scale.

Finally, in preparation for the next figure, note that, while there is similarity, the configurations in Figs. 3d, 3e, and 3f are somewhat shrunken compared with Figs. 3a, 3b, and 3c respectively, indicating that there is a mild tendency toward the clustering of orbits.

Now consider Fig. 4 for which k has been increased to 0.99. In each of these frames, the vertical exaggeration has been fixed at 50. This scaling yields a similarity of the tangent space configurations for this value of k, and indeed, there is a tendency for similarity of the wedges that appear here.

Aside from that, there is such a strong tendency toward the clustering of orbits, i.e., some of the black marks on Figs. 4c and 4d represent 3 or 4 points, that these orbits do not seem to be squeezing down on any kind of curve, even a highly singular one. Something strange is going on at this value of k.

To conclude then, the value of the mean residue, f , determines the value of the residue, R . This, in turn, has a strong influence on the shape of the tangent space figures through Eqs. (23) and (24). The latter fit smoothly against KAM surfaces when k is below the critical value and rumple it nonanalytically at the critical value. Beyond the critical value there is no indication for the existence of KAM surfaces or any other organizing principle.

G Assertion VII

In the previous section, evidence was presented that KAM surfaces existed for values of k up to the critical value. Here we concentrate on showing that stochastic orbits vertically encircling the torus exist for values of k slightly exceeding the critical value. It is clear that horizontally encircling KAM orbits, and vertically encircling stochastic orbits cannot co-exist. It is not so clear that there is no range of k for which neither type of orbit exists. Nevertheless, it appears that this statement is true.

Five orbits are shown in Fig. 5 where k has been chosen to be 0.975. Four of these are periodic, the positive and negative residue points with winding number $144/89$ and $233/144$ respectively. These are the last golden mean convergents for which there are stable orbits. Golden mean convergent orbits with length 377 or greater have residues greater than unity, and are therefore unstable.

A stochastic orbit is also shown on that figure. The initial condition for this orbit was near one of the x points on the figure. The interesting point is that it wanders back and forth

across the region between the periodic orbits, the region where the KAM surface might exist. There is not the slightest indication of an invariant surface in this vicinity that divides phase space.

It was not possible to carry this orbit to the length required for it to encircle the torus vertically. It wandered slowly upward out of the picture, and beyond, but the diffusion of other orbits back into this region is really extraordinarily slow. Similar behavior has been found by Karney¹⁸ in an inhomogeneous random walk problem, showing that it is consistent with a Markovian process.

The details of the stochastic orbit diffusion are governed by a numerical roundoff. One can rapidly lose thousands of digits of formal accuracy in such calculations. To show that the effects of Fig. 5 are not strictly roundoff, we present Fig. 6.

For this figure, k is 0.97. From the criteria of Assertion VI, KAM surfaces exist on both sides of the stochastic orbit shown. The length of the orbit shown in this figure is a few hundred thousand. In another calculation, this orbit was taken to a length of $5 \cdot 10^7$, and it was entirely contained within the stochastic orbit region exhibited here, in spite of the fact that crude estimates show that the calculation suffered from truly fantastic numerical error.

How can this be? A more careful consideration of the numerical error is called for. A detailed calculation of this is given in Appendix C. It turns out that, at a given point, the errors from all the preceding parts of the orbit are, to great accuracy, spread out in only one direction. When this direction is calculated, it is found to be parallel to the apparent edge of the stochastic orbit in Fig. 6. Thus, numerical error can only lead to diffusion parallel

to KAM surfaces, not across them.

As for numerical error in diffusing orbits, other calculations, similar in spirit,^{11,19} have shown that there is almost always one exact orbit in the vicinity of any orbit determined numerically with a roundoff error that is small for each iteration.

These considerations lead to the conclusion that roundoff does not affect the essential features to be learned from Figs. 5 and 6.

V. DISCUSSION

This paper has explored the concept that there is a close relation between the existence of KAM surfaces and the stability of nearby periodic orbits. The relationship has been found to be very close when the problem is put in the proper perspective. In this section we first review that perspective.

Since not all orbits can be calculated and evaluated for stability, a credible method must be found for estimating this trait by extrapolation. Eigenvalues evaluated in the tangent space of the periodic orbit, as in Eqs. (10), (11) and (15), quantitatively characterize the stability of the orbit. These eigenvalues are unsuited for extrapolation, however, because they are not analytic functions of the parameters of the system. They have branch points where they turn from real to complex as in Eq. (11).

Information equivalent to these eigenvalues is contained in the residue, R , defined in Eqs. (10) or (15). This residue is a real continuous function of the parameters of the system. It is, thus, in this respect quite suitable for interpolation and extrapolation.

As a vehicle for extrapolation, the residue suffers from another problem. Orbits near a KAM surface have varying lengths and are longer, the closer the orbit is to the surface. It has been noted by several authors in the past^{11,20,21} that the residue has an exponential dependence on orbit length. The methods of Appendix B of this paper allow this result to be established firmly

for large and small k . As a result, nearby orbits may have vastly different residues. This exponential dependence on orbit length can be suppressed by defining the mean residue in Eq. (17).

Even this mean residue, or residue per unit length, is not a continuous function of relative location of the periodic orbit. More precisely, it does not depend continuously on the winding number q defined in Eq. (3). The problem is that periodic orbits perturb nearby longer periodic orbits. An orbit of given length is more likely to be unstable if it is close to a shorter periodic orbit and more likely to be stable if it is relatively isolated. Since every rational number has its zone of perturbation, the dependence of f on the winding number q is very peculiar as seen for example in Refs. 11 or 21.

One way to deal with this problem is to express the winding number as a continued fraction as was done in Eq. (4). The magnitudes of the partial quotients of the continued fraction provide an estimate of all the perturbations on the given orbit. It is not yet possible to estimate the mean residue, f , quantitatively as a function of these partial quotients, but they do yield a very useful qualitative understanding. This understanding can be used to estimate the stability of orbits by extrapolation of known results for nearby orbits.

In order to relate the existence of a KAM surface to the stability of nearby periodic orbits, it is desirable to make a careful choice of this set of orbits. It should be a sequence of successively longer orbits that asymptotically, in some sense, approach the postulated KAM surface. Further, each member should be as close to the

desired surface as feasible and as far from the perturbing effects of other, shorter orbits. A choice that meets these criteria is the set whose winding numbers are the convergents to the KAM winding number. These were defined in Sec. II.

These considerations determined the calculations made in this paper.

The results of a large number of these numerical calculations has been distilled into a series of assertions in Sec. III.

According to Assertion III, the sequence of mean residues for the convergents of a KAM surface converges to a limit. For the sequences calculated in Sec. IVC, adding a partial quotient had a smaller effect when the continued fraction representation of the winding number had many partial quotients.

When the limiting mean residue is less than one, beyond some orbit length all the residues will be less than one according to Eq. (17). In fact, the residues rapidly approach zero in the limit. Therefore, the positive residue orbits are stable. On the other hand, when the limiting mean residue is greater than one, the converse is true. In this case both the positive and negative residue orbits of the chosen set are unstable for orbits longer than some length.

Figures 2,3, and 4 show graphically that there is a close relation between KAM surfaces and the stability of nearby periodic orbits. Repeating the discussion from Sec. IVF, the environment of an irrational winding number is entirely different depending on whether the nearby periodic orbits are stable or unstable. This is particularly true because, according to Eq. (17), the stability of these orbits is extreme whether stable or unstable. It is thus

reasonable that the value of the converged mean residue for an irrational winding number determines the existence of the corresponding KAM surface. This idea has been discussed in Ref. 21.

Convergence of the mean residue can be optimized by judicious choice of β in Eq. (17). It appears that $\beta = 1/4$ is the preferred value for all cases that have been considered to date. The underlying reason is given in Assertion V. This choice of β yields remarkably good results. For example, consider the crudest approximation to the converged mean residue for the golden mean surface discussed in Sec. III. The leading convergents to this surface are the periodic orbits with q of one and two. The mean residue was evaluated analytically for these orbits in Sec. IVA and is equal to k in either case. Thus, the leading estimate for the converged mean residue of the golden mean surface is

$$f(q_n^*) \approx k.$$

This estimate yields a critical k of unity, only a few percent different from the more exact value of Assertion VII! So, the method described in this paper seems well suited for giving rough estimates for stochastic behavior

The accuracy of this estimate depends critically on choosing an optimum value of β in Eq. (17). That is, it depends on Assertion V, that near the critical k many orbits have residues near $1/4$. It is interesting to examine this criterion geometrically. From Eq. (14), the corresponding value of α for these orbits is 60° . When a periodic orbit bifurcates out an orbit with period six times longer than itself, some nearby related KAM surface is on the

edge of disappearance. This relationship has been noted by Lichtenberg²² also.

Sufficient numerical work has been done on this problem to identify reasonable hypotheses, but considerable effort is now needed to provide proofs. Probably the most crucial of these is Assertion III, concerning the convergence of the mean k residue for irrational winding numbers. It might be possible to use the methods of Appendix B to establish this hypothesis for small k as a first step. Such a proof would show that the mean residue is indeed a fruitful concept.

ACKNOWLEDGMENTS

The author is particularly indebted to Drs. Bountis and Helleman for sharing their insights. Their help in pointing the way toward the calculation of Appendix B is especially appreciated. This paper has also benefited greatly from discussions with many people among whom are Drs. Kruskal, Moser, Kaufman, Lichtenberg, Meiss, Treve, Karney, Dewar, Oberman, Krommes, Rechester, and Finn. The hospitality of the Lawrence Livermore Laboratory, where part of this paper was written, was very helpful. Finally, the support and encouragement of Dr. Ford has been greatly appreciated.

This work was supported by the United States Department of Energy Contract No. EY-76-C-02-3073.

APPENDIX A: Calculation of Periodic Orbits

It is possible to use the symmetry of the mapping to reduce the problem of finding a given periodic orbit to one of finding the root of a function of one variable. This reduction from a two-dimensional problem to a one-dimensional problem vastly increases the speed and accuracy with which these orbits can be determined. This method has been described thoroughly by deVogeleare²³ but is included here for completeness.

The nature of the symmetry can be stated succinctly: the mapping is the product of two involutions. In other words, if the standard mapping is denoted by T , then

$$T = I_2 I_1 \tag{A1}$$

where I_1 is given by

$$\begin{aligned} \theta_n &= -\theta_{n-1} , \\ r_n &= r_{n-1} - \frac{k}{2\pi} \sin 2\pi \theta_{n-1} , \end{aligned} \tag{A2}$$

and I_2 by

$$\begin{aligned} \theta_{n+1} &= -\theta_n + r_n , \\ r_{n+1} &= r_n . \end{aligned} \tag{A3}$$

It is straightforward to show that

$$I_1^2 = 1 \quad , \quad I_2^2 = 1 \quad , \quad (A4)$$

so that these transformations are involutions.

Each of these involutions has lines of fixed points. Namely,

$$I_1(r, \theta) = (r, \theta)$$

is satisfied by $\theta = 0$ or $\theta = 1/2$ for any r , and

$$I_2(r, \theta) = (r, \theta)$$

is satisfied by $\theta = \frac{1}{2}r$ or $\theta = \frac{1}{2}(r+1)$

It is now easy to show that if the initial value of an orbit is a fixed point of I_1 ,

$$I_1(r_0, \theta_0) = (r_0, \theta_0) \quad , \quad (A5)$$

and the N^{th} iterate is also a fixed point of I_1 ,

$$I_1 T^N(r_0, \theta_0) = T^N(r_0, \theta_0) \quad , \quad (A6)$$

then the full orbit is periodic with length $2N$. Consider with the aid of Eqs. (A1), (A5) and (A6),

$$T^{2N}(r_0, \theta_0) = T^{N-1} I_2 I_1 T^{N-1} I_2 I_1(r_0, \theta_0) = T^{N-1} I_2 T^{N-1} I_2(r_0, \theta_0) \quad . \quad (A7)$$

From Eqs. (A1) and (A4),

$$I_2 T = I_1, \quad T I_1 = I_2 \quad (A8)$$

which, used alternately in Eq. (A7) yields

$$T^{2N}(r_0, \theta_0) = (r_0, \theta_0) \quad (A9)$$

as stated.

Thus, the problem of finding periodic orbits has been reduced to that of finding the root of any function that vanishes on the fixed lines of I_1 , and with the independent variable taken to be the one parameter family of fixed points of I_1 . For example, fixed points can be found from the solutions of

$$\sin 2\pi \theta_N(r_0) = 0$$

with $\theta_0 = 0$.

The procedure can be readily generalized to include the fixed points of I_2 as either the initial or the final point of the computed orbit. All the periodic orbits that exist down to $k=0$ can be determined this way.

APPENDIX B: Expansion for Small k

In this Appendix an algorithm is derived for calculating the residue, R , in the limit of small k . It is shown that R is proportional to k^Q , where Q is the length of the periodic orbit. In the first few paragraphs, the relation between the two forms for calculating R , Eqs. (10) and (15), is derived, since the less familiar Bountis and Helleman¹² form is used in the argument of this Appendix.

The equations governing the orbits in the tangent space are found by differencing Eq. (1) and evaluating the coefficients on the periodic orbit considered, yielding

$$\begin{aligned}\delta r_{n+1} &= \delta r_n - k \cos 2\pi \theta_n \delta \theta_n, \\ \delta \theta_{n+1} &= \delta \theta_n + \delta r_{n+1},\end{aligned}\tag{B1}$$

where θ_n is the coordinate of the n^{th} point on the periodic orbit. A set of equations for the $2Q$ variables $(\delta \theta_1, \delta r_1, \dots, \delta \theta_Q, \delta r_Q)$ is closed through the Floquet condition,

$$\begin{aligned}\delta r_{n+Q} &= \lambda \delta r_n, \\ \delta \theta_{n+Q} &= \lambda \delta \theta_n.\end{aligned}\tag{B2}$$

Then $(\delta r_Q, \delta \theta_Q)$ is an eigenvector of M of Eqs. (7) and (8), with eigenvalue λ .

These equations can be written in matrix form

$$\begin{pmatrix}
 1 & 0 & -1 & 1 & 0 & 0 & \dots \\
 -k \cos 2\pi \theta_1 & 1 & 0 & -1 & 0 & 0 & \dots \\
 0 & 0 & 1 & 0 & -1 & 1 & \dots \\
 0 & 0 & -k \cos 2\pi \theta_2 & 1 & 0 & -1 & \dots \\
 \vdots & \vdots & \vdots & \vdots & \vdots & \vdots & \vdots \\
 -\lambda & \lambda & 0 & 0 & \dots & 1 & 0 \\
 0 & -\lambda & 0 & 0 & \dots & -k \cos 2\pi \theta_Q & 1
 \end{pmatrix}
 \begin{pmatrix}
 \delta \theta_1 \\
 \delta r_1 \\
 \delta \theta_2 \\
 \delta r_2 \\
 \vdots \\
 \delta \theta_Q \\
 \delta r_Q
 \end{pmatrix}
 = \underline{\underline{J}} \cdot \underline{\delta x} = 0 \quad .$$

(B3)

The condition that the determinant of $\underline{\underline{J}}$ vanishes yields an equation for λ .

Adding each even numbered row to the row above yields

$$\text{Det } \underline{\underline{J}} = \text{Det } \begin{pmatrix}
 M_1 & -1 & 0 & 0 & \dots \\
 0 & M_2 & -1 & 0 & \dots \\
 \vdots & \vdots & \vdots & \vdots & \vdots \\
 \vdots & \vdots & \vdots & \vdots & \vdots \\
 -\lambda & 0 & \dots & \dots & M_Q
 \end{pmatrix}$$

(B4)

where each element is now a 2×2 matrix, and

$$M_i = \begin{pmatrix} 1 - k \cos 2\pi \theta_i & 1 \\ -k \cos 2\pi \theta_i & 1 \end{pmatrix} \quad .$$

(B5)

Multiplying the first row by M_2 , and adding the second row, and continuing on to eliminate all but the diagonal term in the first row, we find

$$\text{Det } \underline{J} = \text{Det} \left(\prod_{i=1}^Q M_i - \lambda I \right) \quad (\text{B6})$$

where $\text{Det } M_1 = 1$ has been used. This is the usual equation for the eigenvalue λ .

Alternatively, the fourth element in the first row of Eq. (B3) can be used to eliminate every other element in its row and column. The other 1's down that diagonal are treated similarly, as is the λ in the second column next to last row. These elements can then be factored out of the determinant,¹² leaving

$$\text{Det } H(\lambda) = 0 \quad (\text{B7})$$

where

$$H(\lambda) = \begin{pmatrix} 2 - k \cos 2\pi \theta_1 & -1 & \dots & -\lambda^{-1} \\ -1 & 2 - k \cos 2\pi \theta_2 & -1 & \dots \\ \vdots & \vdots & \vdots & \\ -\lambda & \dots & -1 & 2 - k \cos 2\pi \theta_Q \end{pmatrix} \quad (\text{B8})$$

is a tridiagonal matrix with additional elements in the corners. Considering the cofactor of the element, λ , yields the result

$$\text{Det } H(\lambda) = \text{Det } H(1) - \lambda - \lambda^{-1} + 2 \quad (\text{B9})$$

Since the residue R is related to the eigenvalue λ , we obtain directly

$$R = -\frac{1}{4} \text{Det } H(1) \quad . \quad (B10)$$

In some respects, a determinant is easier to calculate than the trace of a product.

The relation between these two forms for calculating R is analogous to the relation between Hill's method and the shooting method for calculating the Floquet parameter for the Mathieu equation.

We now proceed to evaluate $\text{Det } H(1)$. The argument $\lambda = 1$ will be understood for the rest of this section, and thus dropped from the notation. At $k = 0$,

$$H(k=0) = \begin{pmatrix} 2 & -1 & 0 & \dots & -1 \\ -1 & 2 & -1 & \dots & \\ 0 & -1 & 2 & \dots & \\ \vdots & & & & \\ -1 & \dots & & & -1 & 2 \end{pmatrix} \quad . \quad (B11)$$

It can be seen immediately that the eigenvalues of this matrix are

$$\eta_j = 2(1 - \cos 2\pi j/Q) = 4 \sin^2 \pi j/Q \quad (B12)$$

with eigenvectors,

$$a_{n,j} = \cos 2\pi n j/Q \quad . \quad (B13)$$

The lowest eigenvalue vanishes, so

$$\text{Det } H(k=0) = 0 \quad . \quad (B14)$$

The product of the others can be evaluated with the result²⁴

$$\prod_{j=1}^{Q-1} \eta_j = Q^2 \quad . \quad (B15)$$

It follows from $\text{Det } H = \prod_j \eta_j$ that the lowest order nonvanishing approximation to $\text{Det } H$ is $Q^2 \eta_0$, where η_0 is the lowest order nonvanishing approximation to the lowest eigenvalue of the symmetric matrix H .

Since H depends on the orbits, it is necessary to evaluate the orbits to some degree of accuracy. It will be shown by the result that the requisite order is k^{Q-1} .

The coordinate r_n can be eliminated from the standard mapping, Eq. (1), yielding

$$-\theta_{n+1} + 2\theta_n - \theta_{n-1} = \frac{k}{2\pi} \sin 2\pi \theta_n \quad . \quad (B16)$$

This has been written in recursion form. That is, if the periodic orbit is known to some degree of precision, and that estimate is used to evaluate the right-hand side of Eq. (B16), inverting the operator on the left yields an estimate improved by one order in k . The inversion is done with the periodicity condition

$$\theta_{n+Q} = \theta_n \quad . \quad (B17)$$

We already know something about this operator, since it is $H(k=0)$. For one thing it is singular, and each element of the eigenvector of the vanishing eigenvalue is unity. Multiplying by this eigenvector yields the solvability condition

$$\sum_{n=1}^Q \sin 2\pi \theta_n = 0 \quad . \quad (B18)$$

A formal solution of these equations can be written in the form

$$2\pi \theta_n = 2\pi \theta_n^{(0)} + \sum_{j=0}^{\infty} \sum_{\ell=1}^Q \frac{a_{\ell j} (r^{(0)})^{\ell+2j}}{2(1-\cos 2\pi \ell r^{(0)})} \sin 2\pi \ell \theta_n^{(0)} \quad (B19)$$

where

$$r^{(0)} \equiv P/Q \quad ,$$

$$\theta_{n+1}^{(0)} = \theta_n^{(0)} + r^{(0)} \quad , \quad (B20)$$

P and Q are relatively prime, $\theta_0^{(0)}$ will be determined later, and the $a_{\ell j}$ coefficients are evaluated as follows. Inserting this form into the right- and left-hand sides of Eq. (B16) yields

$$\begin{aligned} \sum_{j=0}^{\infty} \sum_{\ell=1}^Q a_{\ell j} k^{\ell+2j} \sin 2\pi \ell \theta_n^{(0)} &= k \sin 2\pi \theta_n \\ &= k \sin \left[2\pi \theta_n^{(0)} + \sum_{j=0}^{\infty} \sum_{\ell=1}^Q \frac{a_{\ell j} k^{\ell+2j}}{2(1-\cos 2\pi \ell r^{(0)})} \sin 2\pi \ell \theta_n^{(0)} \right] \quad . \end{aligned} \quad (B21)$$

The sine on the right can be expanded since the second term of its argument is small in powers of k . The factors of resulting products are combined to yield Fourier coefficients of $\sin 2\pi \ell \theta_n^{(0)}$ as powers of k . These determine the coefficients $a_{\ell j}$ on the left-hand side, order by order in k . Thus, the formal solution is consistent.

Since from Eq. (B20), the $\theta_n^{(0)}$ are equally spaced in the interval $(0,1)$, the solvability condition is satisfied trivially for $\ell \neq Q$ and thus, up to the order of k^Q . At the order k^Q , the value of $\theta_0^{(0)}$ must be chosen so that $\sin 2\pi Q \theta_n^{(0)} = 0$. There are two such solutions, with $\cos 2\pi Q \theta_n^{(0)} = \pm 1$. With this solvability condition, the problem of a vanishing denominator, $1 - \cos 2\pi \ell r^{(0)}$, disappears. Further, it can be used to eliminate terms with $\ell > Q$ in favor of terms with $\ell < Q$.

Since the relation between the $\theta_n^{(0)}$ and $r^{(0)}$ is identical to the integral mapping for $k=0$, and also from the fact that the solvability condition is satisfied in the lower orders by every point on the surface $r^{(0)} = \text{const.}$, it is apparent that the formal solution above is equivalent to the transformation from an integrable mapping to one that is integrable to all orders. This is useful below so it will be pursued further here.

Consider the transformation

$$r = r(r^{(0)}, \theta^{(0)}) ,$$

$$\theta = \theta(r^{(0)}, \theta^{(0)}) .$$

(B22)

If these functions satisfy

$$\begin{aligned} r(r^{(0)}, \theta^{(0)}) &= \theta(r^{(0)}, \theta^{(0)}) - \theta(r^{(0)}, \theta^{(0)} - r^{(0)}) \\ &\quad - \theta(r^{(0)}, \theta^{(0)} + r^{(0)}) + 2\theta(r^{(0)}, \theta^{(0)}) - \theta(r^{(0)}, \theta^{(0)} - r^{(0)}) \\ &= \frac{k}{2\pi} \sin 2\pi \theta(r^{(0)}, \theta^{(0)}) \end{aligned} \quad (B23)$$

to all orders in k , then $r^{(0)}$ is a constant of the standard mapping to all orders. Eliminating $\theta^{(0)}$ between r and θ would yield an implicit expression for the invariant $r^{(0)}$.

Indeed, the formal solution of these equations is very similar to that given above,

$$2\pi \theta = 2\pi \theta^{(0)} + \sum_{j=0}^{\infty} \sum_{\ell=1}^{\infty} \frac{a_{\ell j} (r^{(0)}) k^{\ell+2j}}{2(1 - \cos 2\pi \ell r^{(0)})} \sin 2\pi \ell \theta^{(0)} \quad (B24)$$

where

$$\begin{aligned} \sum_{j=0}^{\infty} \sum_{\ell=1}^{\infty} a_{\ell j} k^{\ell+2j} \sin 2\pi \ell \theta^{(0)} &= k \sin \left\{ 2\pi \theta^{(0)} \right. \\ &\quad \left. + \sum_{j=0}^{\infty} \sum_{\ell=1}^{\infty} \frac{a_{\ell j} k^{\ell+2j}}{2(1 - \cos 2\pi \ell r^{(0)})} \sin 2\pi \ell \theta^{(0)} \right\} . \end{aligned} \quad (B25)$$

The subscripts on $\theta^{(0)}$ have been dropped since here θ depends continuously on $\theta^{(0)}$, the sum over ℓ has been extended to infinity, and the condition that $r^{(0)}$ be rational has been dropped. Indeed, it is better if it is not rational!

Now return to the problem of calculating the lowest eigenvalue of H ,

$$H(\delta\theta_n) = \eta_0(\delta\theta_n)$$

where $\delta\theta_n$ is the eigenvector. This also can be expressed in recursion form,

$$-\delta\theta_{n+1} + 2\delta\theta_n - \delta\theta_{n-1} = (\eta_0 + k \cos 2\pi \theta_n) \delta\theta_n \quad (B26)$$

again, yielding the operator $H(k=0)$. The solvability condition is used to determine the eigenvalue,

$$\eta_0 = -k \frac{\sum_{n=1}^Q \delta\theta_n \cos 2\pi \theta_n}{\sum_{n=1}^Q \delta\theta_n} \quad (B27)$$

As will be seen, the lowest order of the eigenvalue is the order of k^Q . Thus, we need to evaluate the eigenvector accurate to the order k^{Q-1} , with η_0 being a higher order term in Eq. (B26).

This can be done directly. Take the derivative of Eq. (B23) with respect to $\theta^{(0)}$, and evaluate it at the points $\theta^{(0)} = \theta_n^{(0)}$ which are the values of Eq. (B20). It can be verified immediately that these derivatives satisfy the same equation as $\delta\theta_n$, and thus,

$$\delta\theta_n = \partial\theta / \partial\theta^{(0)} \Big|_{\theta^{(0)} = \theta_n^{(0)}} \quad (B28)$$

Since the mapping is effectively integrable to the desired order, the eigenvector is merely deformed by the transformation of Eq. (B22).

It then follows immediately that

$$\begin{aligned} \delta \theta_n k \cos 2\pi \theta_n &= \frac{k}{2\pi} \frac{\partial}{\partial \theta} \sin 2\pi \theta_n \Big|_{\theta_n^{(0)}} \\ &= \sum_{j=0}^{\infty} \sum_{\ell=1}^{\infty} \ell a_{\ell j} k^{\ell+2j} \cos 2\pi \ell \theta_n^{(0)}. \end{aligned} \quad (B29)$$

In evaluating the eigenvalue from Eq. (B27), the sum over n vanishes trivially for $\ell < Q$. Thus, the first nonvanishing term is proportional to k^Q . For $\ell = Q$, the cosines are either plus or minus one depending on the orbit as discussed above. Therefore, the eigenvalue has as its lowest nonvanishing estimate

$$\eta_0 = \mp a_{Q0} Q k^Q, \quad (B30)$$

yielding for the residue

$$R = \pm \frac{1}{4} a_{Q0} Q^3 k^Q. \quad (B31)$$

The quantities a_{Q0} can be calculated one by one using Eq. (B25). It would be exceedingly interesting to know some general properties of these coefficients.

APPENDIX C: Stretching and Numerical Errors

In numerical work, it has been noticed that computed orbits are stochastic only in regions where stochasticity is expected and lie on surfaces when the mapping is integrable. This is surprising in the sense that there are huge numerical errors in calculating these orbits, yet these errors do not seem to fundamentally change the character of the orbit. A part of that question is examined in this Appendix.

These numerical errors are highly anisotropic. Here, we show that errors are generally parallel to KAM surfaces and do not lead to diffusion across them.

Consider a long segment of an orbit that is not periodic. There will be a certain small numerical error in calculating the first iteration of the mapping from (r_1, θ_1) to (r_2, θ_2) . This error will have a probability distribution that can be crudely represented by a small circle. At the end of the considered segment, at the point (r_n, θ_n) , this circle will have become an ellipse, in the tangent space approximation, with a large aspect ratio. Thus, a small error will have become a large error in one direction.

First, let us calculate this ellipse. If the tangent space orbits are represented by

$$\begin{pmatrix} \delta \theta_n \\ \delta r_n \end{pmatrix} = N_{n,2} \begin{pmatrix} \delta \theta_2 \\ \delta r_2 \end{pmatrix} \quad (C1)$$

where the notation distinguishes the matrix N from the similar matrix for periodic orbits, M , then the initial values, and the adjoints, are given in terms of the endpoints by

$$\begin{aligned}\delta \underline{x}_0 &= N_{n,2}^{-1} \delta \underline{x}_n, \\ \delta \underline{x}_0^\dagger &= \delta \underline{x}_n^\dagger (N_{n,2}^{-1})^\dagger.\end{aligned}\tag{C2}$$

The condition that the initial point lie on a circle of radius one,

$$\begin{aligned}\delta \underline{x}_0^\dagger \cdot \delta \underline{x}_0 &= \delta \underline{x}_n^\dagger (N_{n,2}^{-1})^\dagger N_{n,2}^{-1} \delta \underline{x}_n \\ &= \delta r_0^2 + \delta \theta_0^2 \\ &= 1\end{aligned}\tag{C3}$$

yields an expression for the ellipse at (r_n, θ_n) . Thus, the axes of the ellipse are given in terms of the eigenvalues and eigenvectors of $(N_{n,2}^{-1})^\dagger N_{n,2}^{-1}$, or its inverse, NN^\dagger . If N is parameterized

$$N_{n,2} = \begin{pmatrix} a_2 + d_2 & c_2 + b_2 \\ c_2 - b_2 & a_2 - d_2 \end{pmatrix}\tag{C4}$$

with

$$a_2^2 + b_2^2 - c_2^2 - d_2^2 = 1\tag{C5}$$

then

$$N_{n,2} N_{n,2}^\dagger = \begin{pmatrix} A_2 + D_2 & C_2 \\ C_2 & A_2 - D_2 \end{pmatrix}\tag{C6}$$

where

$$\begin{aligned} A_2 &= a_2^2 + b_2^2 + c_2^2 + d_2^2 \\ C_2 &= 2(a_2 c_2 - b_2 d_2) \\ D_2 &= 2(a_2 d_2 + b_2 c_2) \end{aligned} \quad (C7)$$

The eigenvalues of this matrix are the squares of the major and minor semi-axes,

$$\begin{aligned} \rho_{\pm}^2 &= A_2 \pm (A_2^2 - 1)^{1/2} \\ &= [(a_2^2 + b_2^2)^{1/2} \pm (c_2^2 + d_2^2)^{1/2}]^2 \end{aligned} \quad (C8)$$

and the eigenvectors yield the angle, θ_e , that this ellipse makes with the line $\delta r = 0$,

$$\tan \theta_e = C_2 / [(A_2^2 - 1)^{1/2} + D_2] \quad (C9)$$

Note that the eigenvalues of the matrix $N_{n,2}$ do not enter, and in fact this result depends on both a_2 and b_2 whereas the eigenvalues of $N_{n,2}$ depend only on a_2 . Nor is there any reason for eigenvalues to be important. They are appropriate for determining the properties of powers of $N_{n,2}$ and the nonperiodic orbit will never retrace this orbit segment.

Next consider the effect of the roundoff error that arises in computing (r_1, θ_1) from (r_0, θ_0) . This error is propagated to the point (r_n, θ_n) over a slightly longer path, so the corresponding orbits in the tangent space are given by

$$N_{n,1} \equiv \begin{pmatrix} a_1 + d_1 & c_1 + b_1 \\ c_1 - b_1 & a_1 - d_1 \end{pmatrix} = N_{n,2} \begin{pmatrix} a + d & c + b \\ c - b & a - d \end{pmatrix}$$

where the second factor on the right propagates the tangent space orbits from (r_0, θ_0) to (r_1, θ_1) .

Straightforward multiplication yields

$$\begin{aligned} a_1 &= aa_2 - bb_2 + cc_2 + dd_2 \\ b_1 &= ab_2 + ba_2 + cd_2 - dc_2 \\ c_1 &= ac_2 + bd_2 + ca_2 - db_2 \\ d_1 &= ad_2 - bc_2 + cb_2 + da_2 \end{aligned} \quad (C10)$$

and

$$\begin{aligned} a_1 c_1 - b_1 d_1 &= (ac - bd) (a_2^2 - b_2^2 + c_2^2 - d_2^2) \\ &\quad - 2(ad + bc) (a_2 b_2 - c_2 d_2) \\ &\quad + (a^2 + b^2 + c^2 + d^2) (a_2 c_2 - b_2 d_2) \\ a_1 d_1 + b_1 c_1 &= 2(ac - bd) (a_2 b_2 + c_2 d_2) \\ &\quad + (ad + bc) (a_2^2 - b_2^2 - c_2^2 + d_2^2) \\ &\quad + (a^2 + b^2 + c^2 + d^2) (a_2 d_2 + b_2 c_2) \quad . \quad (C11) \end{aligned}$$

We next need some identities that follow from the determinant condition, $a^2 + b^2 = c^2 + d^2 + 1$,

$$\begin{aligned}
 a^2 - b^2 + c^2 - d^2 &= 2(ac - bd) \frac{ac+bd}{a^2+b^2} + \frac{a^2-b^2}{a^2+b^2} \\
 ab - cd &= -(ac - bd) \frac{ad-bc}{a^2+b^2} + \frac{ab}{a^2+b^2} \\
 ab + cd &= (ad + bc) \frac{ac+bd}{a^2+b^2} + \frac{ab}{a^2+b^2} \\
 a^2 - b^2 - c^2 + d^2 &= 2(ad + bc) \frac{ad-bc}{a^2+b^2} + \frac{a^2-b^2}{a^2+b^2} \quad . \quad (C12)
 \end{aligned}$$

Using these results in Eq. (C11) yields

$$a_1 c_1 - b_1 d_1 = (a_2 c_2 - b_2 d_2) S + (ac - bd) \frac{a_2^2 - b_2^2}{a_2^2 + b_2^2} - (ad + bc) \frac{2a_2 b_2}{a_2^2 + b_2^2} \quad (C13)$$

$$a_1 d_1 + b_1 c_1 = (a_2 d_2 + b_2 c_2) S + (ac - bd) \frac{2a_2 b_2}{a_2^2 + b_2^2} + (ad + bc) \frac{a_2^2 - b_2^2}{a_2^2 + b_2^2} \quad (C14)$$

$$a_1^2 + b_1^2 = (a_2^2 + b_2^2) S - (c^2 + d^2) \quad (C15)$$

where

$$S \equiv a^2 + b^2 + c^2 + d^2 + 2(ac - bd) \frac{a_2 c_2 + b_2 d_2}{a_2^2 + b_2^2} + 2(ad + bc) \frac{a_2 d_2 - b_2 c_2}{a_2^2 + b_2^2} \quad . \quad (C16)$$

We are interested in the cases $a_1^2 + b_1^2$ and $a_2^2 + b_2^2$ are both large, so that the ellipses for both roundoff errors are very long, but the coefficients a, b, c and d are not large since the latter only carry the tangent space orbits over one iteration. It follows

from Eq. (C15) that S can not be very small. It also follows from $\text{Det } NN^\dagger = 1$ that at least one of the factors $a_2 c_2 - b_2 d_2$ and $a_2 d_2 + b_2 c_2$ must be large. The two terms on the right of Eqs. (C13) and (C14) can not be large. Hence, the two error ellipses must be very nearly parallel in the limit of interest.

It follows that the large accumulated errors at a given point are all in a direction that is characteristic of the given point. Errors perpendicular to this direction are only of the order of the round-off, and thus, very small. Since the quantity $(a^2 + b^2)$ generally grows exponentially with the orbit length, numerical convergence to the characteristic direction is quite rapid.

These quantities can be calculated on a KAM surface. Since this surface can be transformed to $r^{(0)} = \text{const}$ as in Appendix B, the tangent space orbit can be written in the space $(\delta r^{(0)}, \delta \theta^{(0)})$,

$$N_{n,1} = \begin{pmatrix} 1 & 0 \\ s & 1 \end{pmatrix}^n = \begin{pmatrix} 1 & 0 \\ ns & 1 \end{pmatrix} . \quad (\text{C17})$$

Thus, here $(a^2 + b^2)^{1/2}$ grows only linearly with n . From Eq. (C9), θ_e goes to zero in the limit of large n , so that the roundoff error is parallel to the KAM surface. Numerical calculations confirm this result for orbits that come close to KAM surfaces.

REFERENCES

- ¹M. Hénon and C. Heiles, *Astron. J.* 69, 73 (1964).
- ²J. Ford, in Fundamental Problems in Statistical Mechanics III, edited by E.D.G. Cohen, (North Holland, Amsterdam, 1975), p. 215.
- ³K.J. Whiteman, *Rep. Prog. Phys.* 40, 1033 (1977).
- ⁴B.V. Chirikov, *Phys. Repts.* (to be published).
- ⁵M.V. Berry, in Topics in Nonlinear Dynamics, edited by S. Jorna, *Am. Inst. Phys. Conf. Proc.*, (A.I.P., New York, 1978), Vol. 46.
- ⁶Y.M. Treve, in Topics in Nonlinear Dynamics, edited by S. Jorna, *Am. Inst. Phys. Conf. Proc.* (A.I.P., New York, 1978), Vol. 46.
- ⁷J.B. Taylor, unpublished (1968).
- ⁸V.I. Arnol'd and A. Avez, Ergodic Problems of Classical Mechanics (Benjamin, New York, 1968), p. 94.
- ⁹V.I. Arnol'd, *Usp. Mat. Nauk.* 18, 13 (1963) [Russian Mathematical Surveys 18, No. 5,9 (1963)].
- ¹⁰J. Moser, *Nachr. Akad. Wiss. Göttingen II Math.-Physik Kl.* No. 1 (1962).
- ¹¹J.M. Greene, *J. Math. Phys.* 9, 760 (1968).
- ¹²T. Bountis, PhD Thesis, Physics Dept., University of Rochester, N.Y. (1978); T. Bountis and R. H. G. Helleman, to be submitted to *J. Math Phys.*; R. H. G. Helleman, in Statistical Mechanics and Statistical Methods, edited by U. Landman, (Plenum Press, N.Y., 1977) p. 343, Eqs. (2.10)-(2.12).

- ¹³I. Niven, Irrational Numbers (Mathematical Association of America, Menasha, WI, 1956).
- ¹⁴C. Froeschlé, Astron and Astrophys. 9, 15 (1970).
- ¹⁵G. Benettin, L. Galgani, and J.-M. Strelcyn, Phys. Rev. A 14, 2338 (1976).
- ¹⁶M. Gardner, Second Scientific American Book of Mathematical Puzzles and Diversions, (Simon and Shuster, New York, 1961).
- ¹⁷J.M.A. Danby, Celest. Mech. 8, 273 (1973).
- ¹⁸C.F.F. Karney, private communication.
- ¹⁹G. Benettin, M. Casartelli, L. Galgani, A. Giorgilli, and J.-M. Strelcyn, Nuovo Cimento 44B, 183 (1978).
- ²⁰L.J. Laslett, E.M. McMillan, and J. Moser, Courant Institute Rept. NYO-1480-101 (unpublished) 1968.
- ²¹G.H. Lundsford and J. Ford, J. Math. Phys. 13, 700 (1972).
- ²²A.J. Lichtenberg, private communication.
- ²³R. deVogelaere, Contributions to the Theory of Nonlinear Oscillations, edited by S. Lefschetz (Princeton University Press, Princeton, 1958), Vol IV, p. 53.
- ²⁴I.S. Gradshteyn and I.M. Ryzhik, Table of Integrals, Series, and Products, (Academic Press, New York, 1965), p. 34.

Table I: Mean Residue for $q = 3$ Orbits

<u>k</u>	<u>f⁺</u>	<u>f⁻</u>
0.5	0.52068	0.52118
1.0	1.54378	1.05081
2.0	2.09494	2.16282
20.0	20.48158	21.44352
21.0	21.48851	22.46472

Table II: Mean Residue for Various Orbits with $k = 1$

<u>q</u>	<u>Q/P</u>	<u>f⁺</u>
{1,1,1,1,1}	8/5	1.0325
{1,1,1,2,1}	11/7	1.0638
{1,1,2,1,1}	12/7	1.0378
{1,2,1,1,1}	11/8	1.1139
{1,1,2,2,1}	17/10	1.0475
{1,2,1,2,1}	15/11	1.1447
{1,2,2,1,1}	17/12	1.0967
{1,2,2,2,1}	24/17	1.1070
{1,1,1,3,1}	14/9	1.1020
{1,1,3,1,1}	16/9	1.0796
{1,3,1,1,1}	14/11	1.2290

Table III: Residues and Mean Residues of
Golden Mean Convergents, $k = 0.971635$

<u>Q/P</u>	<u>f^+</u>	<u>R^+</u>	<u>f^-</u>	<u>R^-</u>
89/55	0.99998014	0.24956	1.000217	-0.25488
144/89	1.00001090	0.25039	1.000158	-0.25574
233/144	0.99999772	0.24987	1.000088	-0.25520
377/233	1.00000177	0.25017	1.000058	-0.25551
610/377	0.99999965	0.24995	1.000034	-0.25528
987/610	1.00000009	0.25002	1.000021	-0.25537

Table IV: Mean Residues of Golden Mean Convergents,
 $k = 0.9$

<u>Q/P</u>	<u>f^+</u>	<u>f^-</u>
55/34	0.92427	0.92428
89/55	0.92409	0.92409
144/89	0.92406	0.92406
233/144	0.92401	0.92401

Table V: Residue for Convergents of

$$q = (143 + \sqrt{5})/38, \quad k = 0.834365$$

<u>Q/P</u>	<u>R⁺</u>
730/191	0.24766
1181/309	0.25166
1911/500	0.24924
3092/809	0.25079
5003/1309	0.24995

Figure Captions

Fig. 1 Five orbits for the standard mapping with $k = 0.97$.

Fig. 2 Golden mean convergent periodic orbits with $k = 0.95$.

In (a) positive and negative residue orbit segments are shown for $q = 55/34$ and $89/55$, that lie in a range of θ , $\delta\theta = 5.2 \cdot 10^{-2}$ and a range of r , $\delta r = 1.1 \cdot 10^{-3}$. In (b) the orbits and ranges are $q = 144/89$ and $233/144$ with $\delta\theta = 2.0 \cdot 10^{-2}$ and $\delta r = 1.65 \cdot 10^{-4}$. In (c) they are $q = 377/233$ and $610/377$ with $\delta\theta = 7.5 \cdot 10^{-3}$ and $\delta r = 2.4 \cdot 10^{-5}$, in (d) $q = 987/610$ and $1597/987$ with $\delta\theta = 2.9 \cdot 10^{-3}$ and $\delta r = 3.5 \cdot 10^{-6}$, in (e) $q = 2584/1597$ and $4181/2584$ with $\delta\theta = 1.1 \cdot 10^{-3}$ and $\delta r = 5.0 \cdot 10^{-7}$, and in (f) $q = 6765/4181$ and $10946/6765$ with $\delta\theta = 4.2 \cdot 10^{-4}$ and $\delta r = 7.5 \cdot 10^{-8}$.

Fig. 3 Golden mean convergent periodic orbits with $k = 0.971635$.

In (a) the orbits and ranges are $q = 55/34$ and $89/55$ with $\delta\theta = 5.2 \cdot 10^{-2}$ and $\delta r = 1.0 \cdot 10^{-3}$, in (b) $q = 144/89$ and $233/144$ with $\delta\theta = 2.0 \cdot 10^{-2}$ and $3.0 \cdot 10^{-4}$, in (c) $q = 377/233$ and $610/377$ with $\delta\theta = 7.5 \cdot 10^{-3}$ and $\delta r = 1.5 \cdot 10^{-5}$, in (d) $q = 987/610$ and $1597/987$ with $\delta\theta = 2.9 \cdot 10^{-3}$ and $\delta r = 4.6 \cdot 10^{-6}$, in (e) $q = 2584/1597$ and $4181/2584$ with $\delta\theta = 1.1 \cdot 10^{-3}$ and $\delta r = 1.4 \cdot 10^{-6}$, and in (f) $q = 6765/4181$ and $10946/6765$ with $\delta\theta = 4.2 \cdot 10^{-4}$ and $\delta r = 7.0 \cdot 10^{-8}$.

Fig. 4 Golden mean convergent orbits with $k = 0.99$. In (a) the orbits and ranges are $q = 55/34$ and $89/55$ with $\delta\theta = 5.0 \cdot 10^{-2}$ and $\delta r = 1.0 \cdot 10^{-3}$, in (b) $q = 144/89$ and $233/144$ with $\delta\theta = 2.0 \cdot 10^{-2}$ and $\delta r = 4.0 \cdot 10^{-4}$, in (c) $q = 377/233$ and $610/377$ with $\delta\theta = 7.5 \cdot 10^{-3}$ and $\delta r = 1.5 \cdot 10^{-4}$, and in (d) $q = 987/610$ with $\delta\theta = 3.5 \cdot 10^{-4}$ and $\delta r = 7.0 \cdot 10^{-6}$. In (e) and (f) orbits of (c) with the two values of q have been plotted separately.

Fig. 5 Orbits near the golden mean with $k = 0.975$. Periodic orbits with positive and negative residues are shown for $q = 144/89$ and $233/144$, together with a segment of a stochastic orbit. The ranges of r and θ in this figure are $\delta\theta = 2.0 \cdot 10^{-2}$ and $\delta r = 2.0 \cdot 10^{-4}$.

Fig. 6 Stochastic orbit for $k = 0.97$. The range of r and θ in this figure is $\delta\theta = 1.0 \cdot 10^{-2}$ and $\delta r = 1.2 \cdot 10^{-4}$.

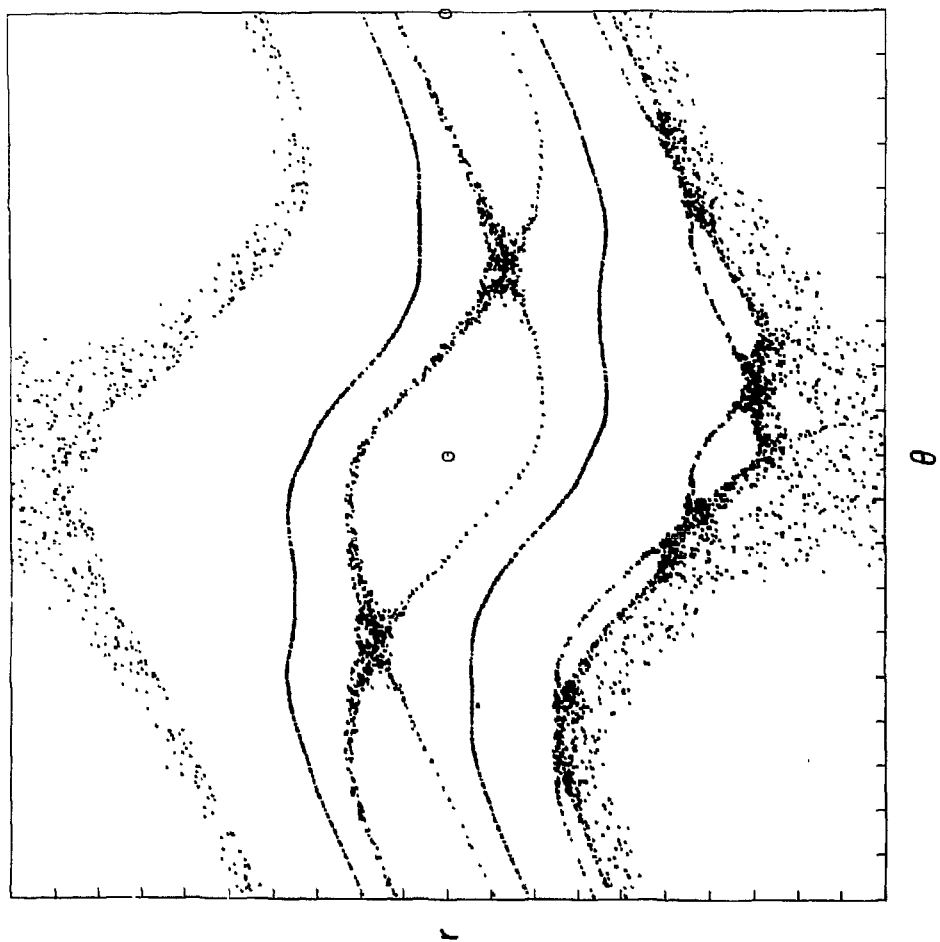


Figure 1.

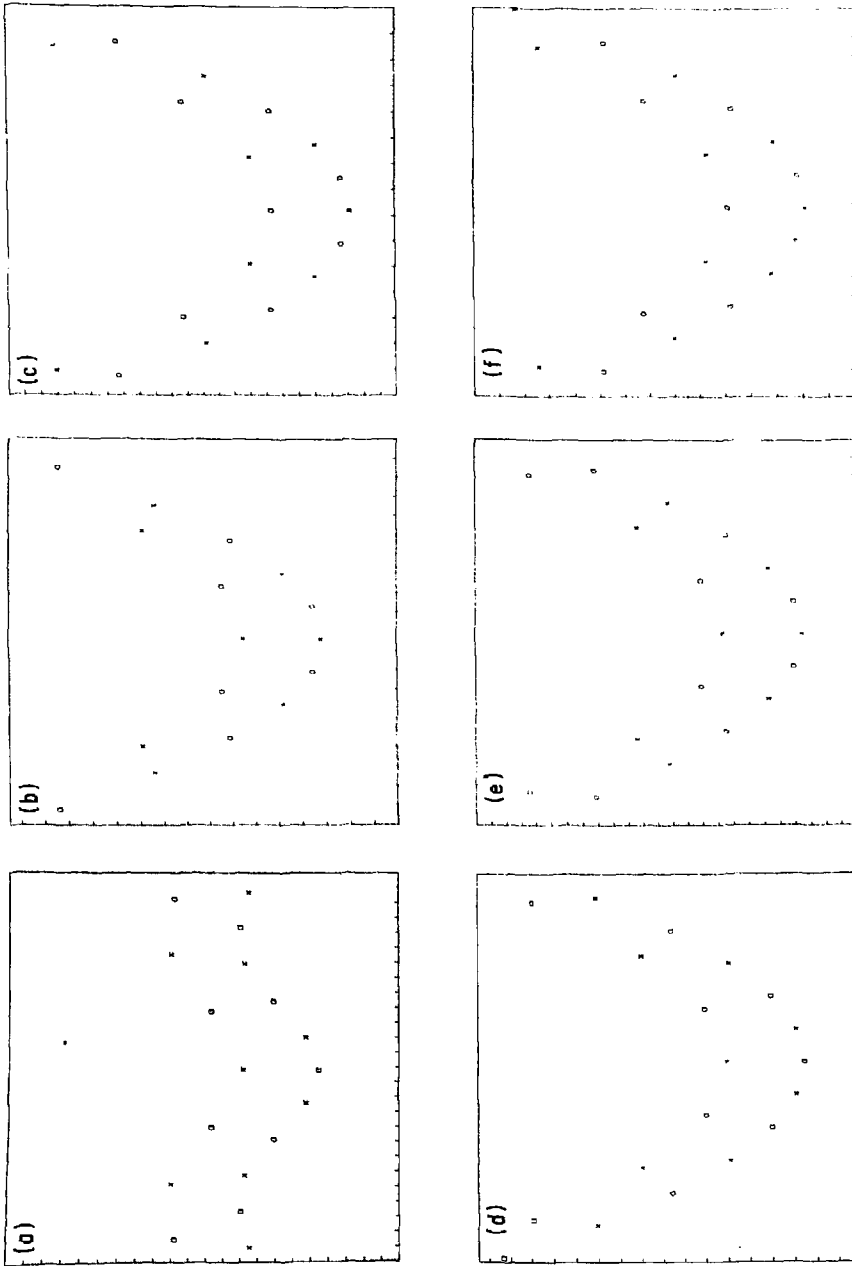


Figure 2. 782212

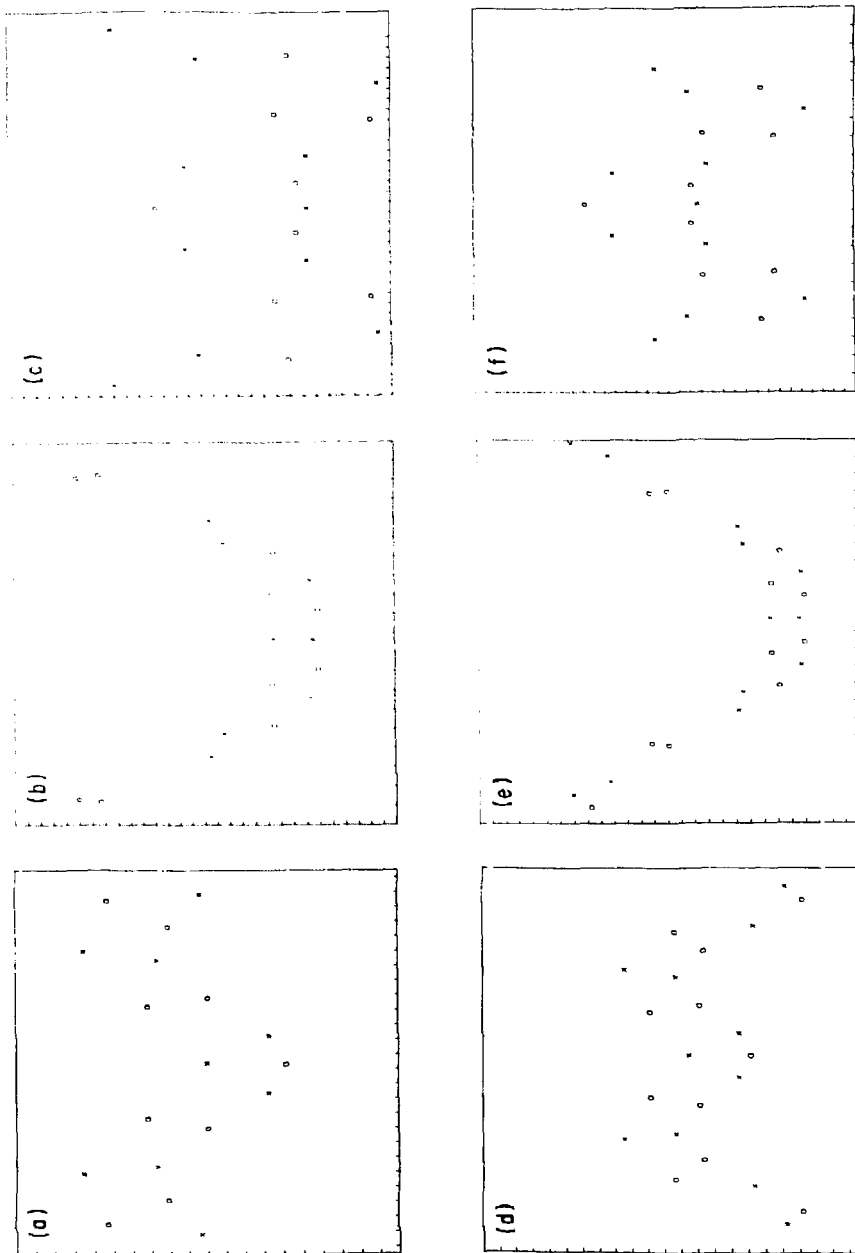


Figure 3. 782211

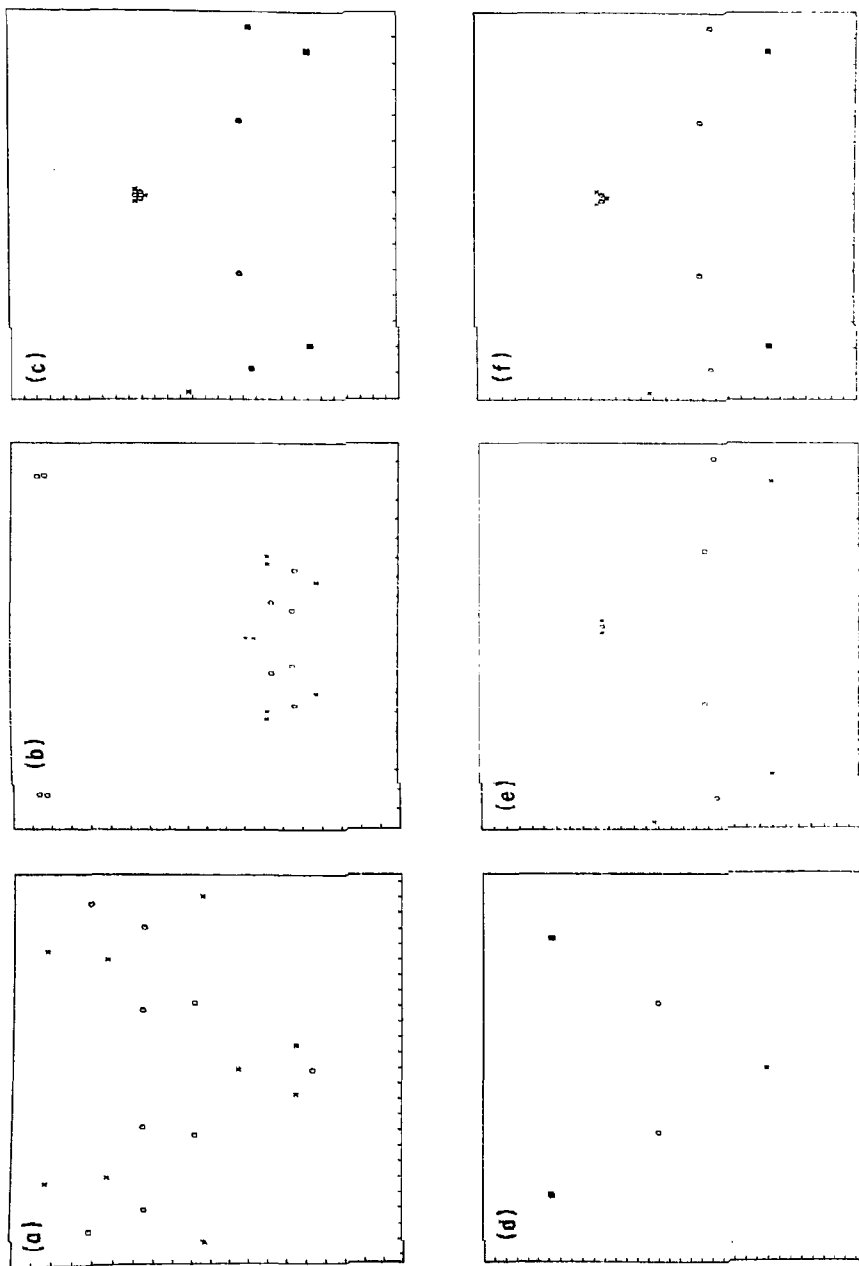


Figure 4. 782210

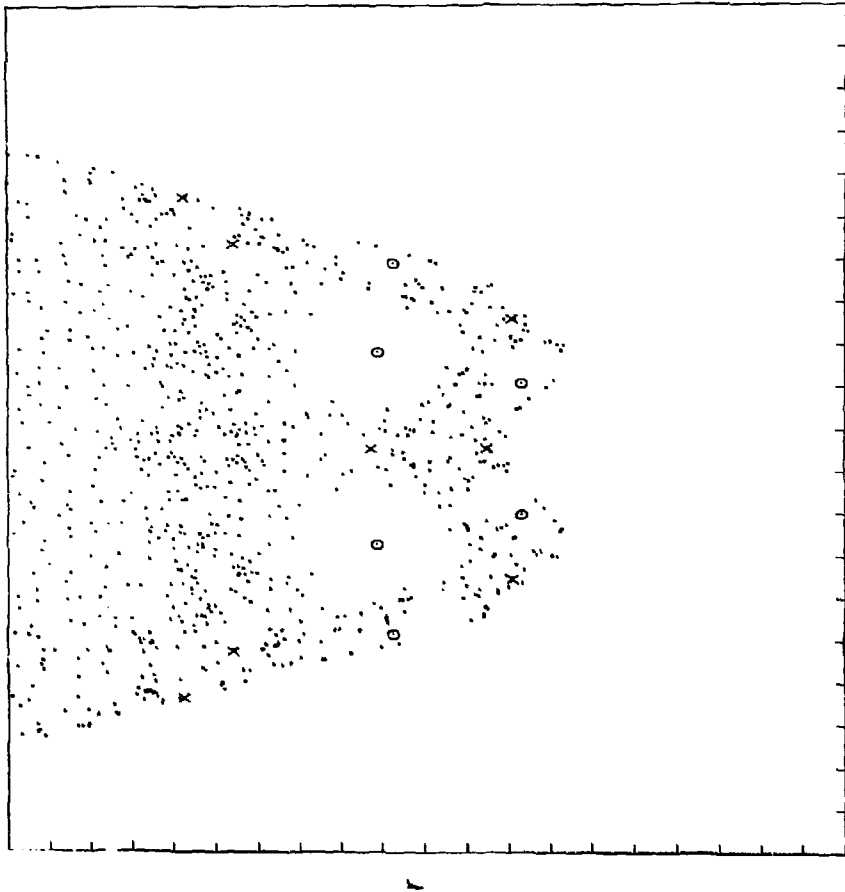


Figure 5.

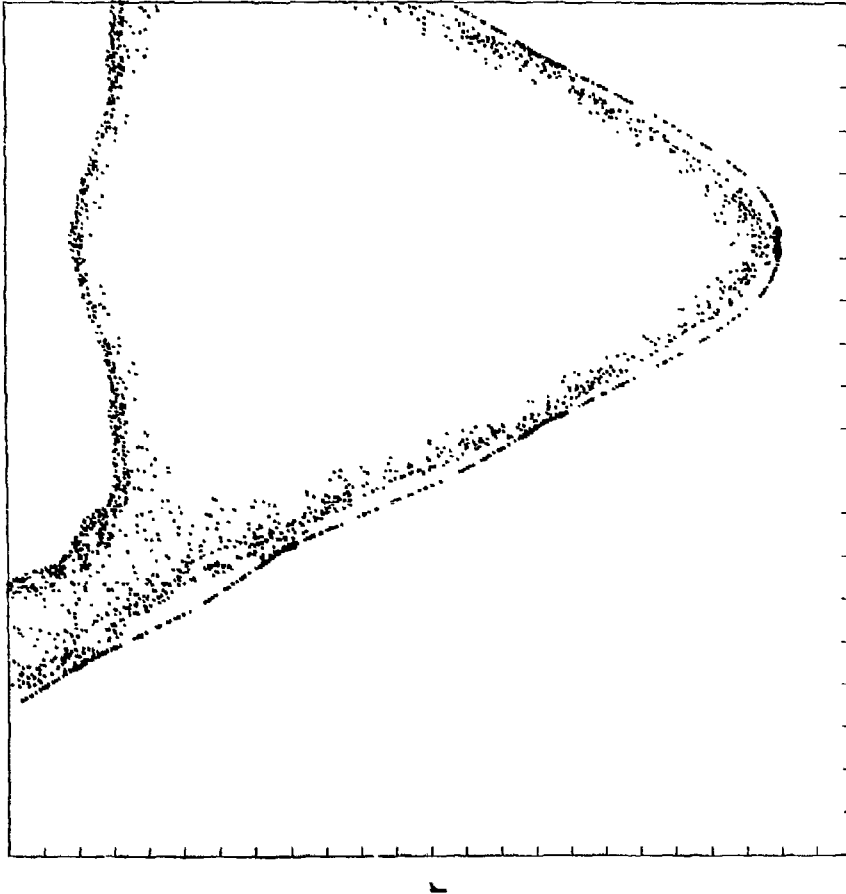


Figure 6.